Multilayer intraclonal heterogeneity in chronic myelomonocytic leukemia

Allan Beke, Lucie Laplane, Julie Riviere, Qin Yang, Miguel Torres-Martin, Thibault Dayris, Philippe Rameau, Veronique Saada, Chrystèle Bilhou-Nabera, Ana Hurtado, et al.

Ferrata Storti Foundation

Haematologica 2020
Volume 105(1):112-123

Multilayer intraclonal heterogeneity in chronic myelomonocytic leukemia

Allan Beke,[1,2,*] Lucie Laplane,[1,3,*] Julie Riviere,[1] Qin Yang,[4] Miguel Torres-Martin,[4] Thibault Dayris,[5] Philippe Rameau,[5] Veronique Saada,[6] Chrystèle Bilhou-Nabera,[7] Ana Hurtado,[8] Larissa Lordier,[1,5] William Vainchenker,[1] Maria E. Figueroa,[4,9] Nathalie Droin[1,2] and Eric Solary[1,2,10]

[1]INSERM U1170, Gustave Roussy Cancer Center, Villejuif, France; [2]Université Paris-Sud, Faculté de Médecine, Le Kremlin-Bicêtre, France; [3]CNRS UMR8590, IHPST, Université Paris 1 Panthéon-Sorbonne, Paris, France; [4]Human Genetics, University of Miami Miller School of Medicine, Miami, FL, USA; [5]CNRS 3655 & INSERM US23, AMMICa, Gustave Roussy Cancer Center, Villejuif, France; [6]Department of Biopathology, Gustave Roussy Cancer Center, Villejuif, France; [7]Service d'Hématologie Biologique, Hôpital Saint-Antoine, Paris, France; [8]Hematology and Medical Oncology Department, Hospital Morales Meseguer, IMIB, Murcia, Spain; [9]Sylvester Comprehensive Cancer Center, University of Miami Miller School of Medicine, Miami, FL, USA and [10]Department of Hematology, Gustave Roussy Cancer Center, Villejuif, France

**AB and LL contributed equally to this study*

ABSTRACT

The functional diversity of cells that compose myeloid malignancies, i.e., the respective roles of genetic and epigenetic heterogeneity in this diversity, remains poorly understood. This question is addressed in chronic myelomonocytic leukemia, a myeloid neoplasm in which clinical diversity contrasts with limited genetic heterogeneity. To generate induced pluripotent stem cell clones, we reprogrammed CD34$^+$ cells collected from a patient with a chronic myelomonocytic leukemia in which whole exome sequencing of peripheral blood monocyte DNA had identified 12 gene mutations, including a mutation in *KDM6A* and two heterozygous mutations in *TET2* in the founding clone and a secondary *KRAS*(G12D) mutation. CD34$^+$ cells from an age-matched healthy donor were also reprogrammed. We captured a part of the genetic heterogeneity observed in the patient, i.e. we analyzed five clones with two genetic backgrounds, without and with the *KRAS*(G12D) mutation. Hematopoietic differentiation of these clones recapitulated the main features of the patient's disease, including overproduction of granulomonocytes and dysmegakaryopoiesis. These analyses also disclosed significant discrepancies in the behavior of hematopoietic cells derived from induced pluripotent stem cell clones with similar genetic background, correlating with limited epigenetic changes. These analyses suggest that, beyond the coding mutations, several levels of intraclonal heterogeneity may participate in the yet unexplained clinical heterogeneity of the disease.

Correspondence:

ERIC SOLARY
eric.solary@gustaveroussy.fr

Received: October 4, 2018.

Accepted: April 30, 2019.

Pre-published: May 2, 2019.

doi:10.3324/haematol.2018.208488

Check the online version for the most updated information on this article, online supplements, and information on authorship & disclosures: www.haematologica.org/content/105/1/112

Introduction

Intratumoral heterogeneity is a major tenet of cancer biology. A tumor clone emerges from a single cell that has acquired one or several somatic mutations. Additional driver events that occur in individual daughter cells generate tumor subclones, each being endowed with specific functional properties and fitness.[1] This intraclonal genetic heterogeneity may not explain all the functional heterogeneity among individual cells within a tumor clone. Epigenetic variation also contributes to the heterogeneity of cells that form a tumor.[2,3]

Chronic myelomonocytic leukemia (CMML) is a neoplastic disease whose limited genetic heterogeneity contrasts with its clinical diversity.[4] CMML is defined by a persistent clonal monocytosis, with or without dysplasia.[5] The mutational landscape contains a small number of somatic mutations in DNA methylation, histone

modifier, splicing factor and signaling genes.[6] Mapping of CMML clonal architecture identified early clonal dominance, intratumor heterogeneity in the hematopoietic stem and progenitor cell compartment in which mutations accumulate mostly linearly, and growth advantage to the most mutated cells.[7] Hypomethylating agents, which are commonly used in severe dysplastic forms of the disease, can restore a balanced hematopoiesis.[8] The response to these drugs, which correlates with DNA demethylation, can occur in the absence of any decrease in mutation allele burden measured in circulating monocytes,[6] arguing for a role of epigenetic alterations in disease expression and outcome.[9]

One of the main limitations in studying CMML pathophysiology is the lack of appropriate models, either patient-derived cell lines or genetically modified animals, which faithfully reproduce disease features. Currently, the best available CMML preclinical model is xenotransplantation of CMML cells in immunocompromised mice, especially those with transgenic expression of human cytokines including granulocyte-macrophage colony-stimulating factor.[10,11] The modeling of myeloid malignancies by generating patient-derived induced pluripotent stem cells (iPSC) recently appeared as another opportunity to model these diseases and, although challenging, capture their genetic heterogeneity.[12–15] In CMML, we previously demonstrated that intraclonal heterogeneity was rarely detected in mature cells of the clone as a consequence of a growth advantage to most mutated cells with differentiation but was preserved in stem and progenitor cells.[6,7] Therefore, we sorted CD34$^+$ cells from a CMML patient and reprogrammed these cells to capture some intraclonal genetic heterogeneity and characterize hematopoiesis derived from genetically close but distinct iPSC.

Methods

Generation, characterization and maintenance of induced pluripotent stem cells

CD34$^+$ cells collected from a healthy donor and a CMML patient, with informed consent and approval of the Ethics Committee (DC-2014-209), were infected with non-integrated Sendai virus encoding Klf4, Oct4, Sox2 and c-Myc to generate iPSC. An additional iPSC (Co6) was kindly provided by Dr Weiss.[16] iPSC were passaged once a week to yield a cell suspension of small colonies (3-10 cells). Intracellular and extracellular pluripotency markers were detected by flow cytometry and teratoma formation was evaluated by intramuscular injection of iPSC into *NOD/SCID/IL2rγ*$^{-/-}$ mice. Karyotyping and comparative genomic hybridization were performed. The procedures are detailed in the *Online Supplementary Material*.

Hematopoietic cell differentiation

A two-dimensional monolayer system was used to differentiate iPSC into CD34$^+$CD43$^+$ hematopoietic progenitor cells (HPC). Clonogenic assays were performed by mixing HPC in serum-free medium with MethoCult H4434 classic (Stem Cell Technologies, Grenoble, France) before plating the cell suspension in 35-mm dishes. Colonies were scored after 14 days and analyzed on a BD LSRFortessa X-20. HPC mixed with serum-free fibrin clots were seeded for 10 days in the presence of thrombopoietin and stem cell factor before measuring colony-forming unit-megakaryocyte (CFU-Mk) colonies. HPC were also suspended in serum-free liquid medium with growth factors for 10 days before flow analysis of cell surface markers and May-Grünwald-Giemsa staining of cytospins. More details are provided in the *Online Supplementary Material*.

Flow cytometry and cell sorting

The antibodies used are listed in *Online Supplementary Table S1*. Cells were analyzed using a BD LSRFortessa™ X-20 and Kaluza analysis software. HPC, monocytes and megakaryocytes were sorted on a BD Influx™ Cell sorter. Details are provided in the *Online Supplementary Material*.

Whole exome sequencing

We collected genomic DNA from sorted monocytes and CD3$^+$ T cells and iPSC to perform whole exome sequencing. Raw reads were aligned to the reference human genome hg19 (Genome Reference Consortium GRCh37) using BWA 0.5.9 (Burrows–Wheeler Aligner) backtrack algorithm with default parameters. A mutation was reported as present if the variant allele frequency was ≥4%. More details are provided in the *Online Supplementary Material*.

Genome-wide DNA methylation detected by enhanced reduced representation bisulfite sequencing

High-molecular weight DNA was sequenced on a HiSeq3000 Illumina sequencer and 50 bp reads were aligned against a bisulfite-converted human genome (hg19). Differentially methylated regions (DMR) identified an absolute methylation difference ≥40% with a false discovery rate <5% and were annotated using the ChIPenrich R package,[17] which was also used for gene ontology and pathway analysis. For correspondence analysis and hierarchical clustering, tiles with the highest standard deviation (SD >0.03) were used. More details are provided in the *Online Supplementary Material*.

Statistical analysis

Statistical analysis was performed with GraphPad Prism software, using an unpaired *t* test and Mann-Whitney test, depending on distribution, similarity of variance, and sample number. The Kruskal-Wallis test was used for multiple comparisons.

Data availability

Accession numbers for enhanced reduced representation bisulfite sequencing, whole exome sequencing and RNA sequencing data are GSE114115, E-MTAB-7917 and E-MTAB-7850, respectively.

Results

Reprogramming of CD34$^+$ cells from a patient with chronic monomyelocytic leukemia captures a part of the disease's genetic heterogeneity

We reprogrammed CD34$^+$ cells collected from a CMML patient whose monocyte DNA whole exome sequencing had identified 12 mutations, including two mutations in *TET2* (S1691fs and R1516X) and heterozygous mutations in *KRAS*(G12D) and *KDM6A*(R61X). The clinical and biological features of the patient's disease are depicted in the *Online Supplementary Material.* Reprogramming of CD34$^+$ cells collected from an age-matched healthy donor generated control clones (Figure 1A, B). We selected nine clones (5 from the patient; 4 from the healthy donor) demonstrating pluripotency features, including morphology (*Online Supplementary Figure S1A*), expression of markers (*Online Supplementary Figure S1B*) and formation of teratomas in

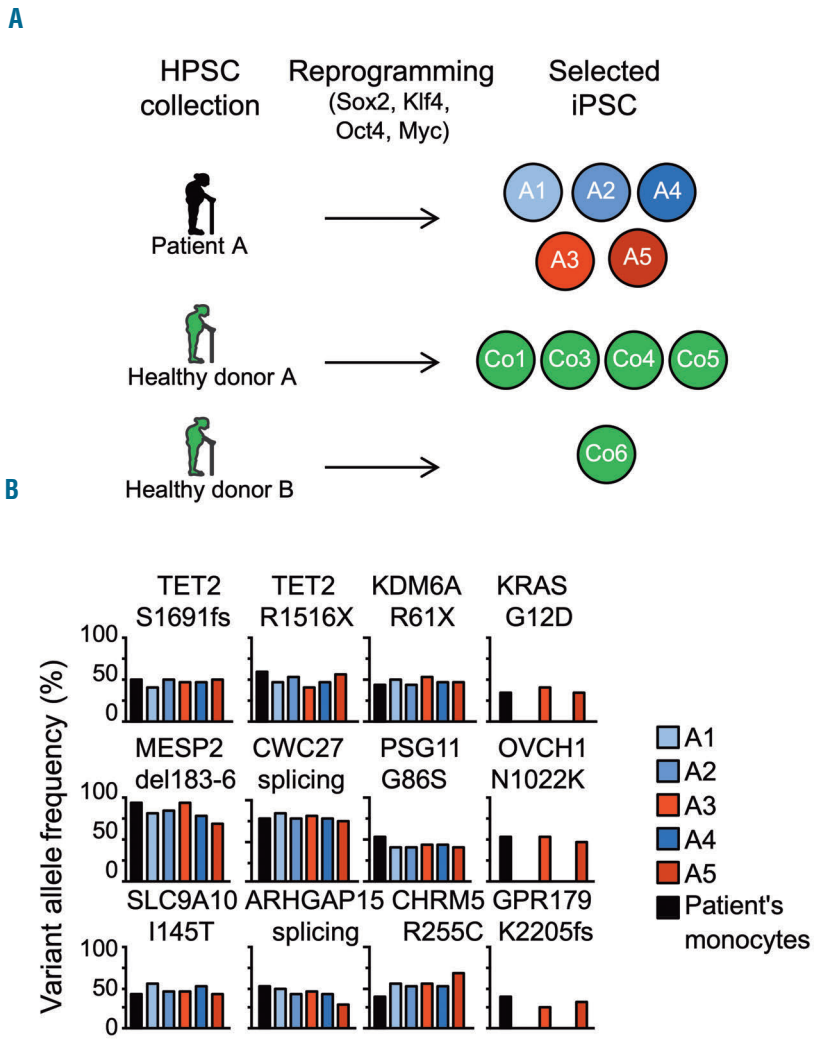

Figure 1. Generation and genetic characterization of chronic myelomonocytic leukemia- and control-induced pluripotent stem cells. (A) CD34$^+$ cells from a patient with chronic myelomonocytic leukemia and an age-matched healthy donor were reprogrammed through infection with Sendai virus encoding the transcription factors Sox2, Klf4, Oct4, and c-Myc (SKOM) before characterization and selection of indicated induced-pluripotent stem clones (iPSC). An additional control iPSC (Co6) was kindly provided by Dr. Weiss. (B) Whole exome sequencing of DNA collected from sorted peripheral blood monocytes (in black) and from five iPSC selected from patient A (each color indicates a specific clone), showing the detection of two genotypes with nine and 12 somatic variants, respectively.

immunodeficient mice (*Online Supplementary Figure S1C*), without reprogramming-induced cytogenetic abnormalities (*Online Supplementary Figure S1D*). We also used an additional, independently generated control clone (Figure 1A).[16] Whole exome sequencing and Sanger sequencing of patient-derived iPSC indicated that we had captured a part of the genetic heterogeneity of her leukemic clone, i.e., three clones (A1, A2, A4) recapitulated the founding clone while the other two (A3, A5) were reprogrammed from a *KRAS*(G12D) subclone (Figure 1A, B and *Online Supplementary Figure S1E*). In contrast with other studies,[18] we did not reprogram any wildtype CD34$^+$ cells, probably due to the early clonal dominance that characterizes CMML clonal architecture, with very few residual wildtype cells in the stem cell compartment.[7]

Hematopoietic cells derived from chronic myelomonocytic leukemia induced pluripotent stem cells recapitulate the disease features

iPSC were induced to differentiate into CD34$^+$CD43$^+$ hematopoietic progenitors (*Online Supplementary Figure S2A*), which were plated for 10 days in methylcellulose in the presence of stem cell factor, interleukin-3, erythropoietin, and granulocyte-macrophage colony-stimulating factor (Figure 2A). The total numbers of colonies generated by healthy donor- and CMML iPSC-derived hematopoietic progenitors were similar (Figure 2B and *Online Supplementary Figure S3A*). The fraction of clusters (colonies <50 cells) generated by *KRAS* wildtype CMML iPSC was significantly higher than that generated by *KRAS*(G12D)-mutated CMML iPSC and control clones (Figure 2C and *Online Supplementary Figure S3B, C*). *KRAS*(G12D) clones produced larger granulocyte-macrophage (CFU-GM) and macrophage (CFU-M) colonies (Figure 2D) as well as a higher proportion of CFU-M colonies (Figure 2E). Compared to control clones, CMML-derived clones generated fewer granulocytic and multipotent progenitor colonies (Figure 2E, F and *Online Supplementary Figure S3D*) and more granulocyte-macrophage colonies (Figure 2E) whereas the proportions of erythroid colonies were not significantly different (Figure 2F and *Online Supplementary Figure S3D*). Colonies derived from CMML iPSC also demonstrated an increased fraction of CD14$^+$ cells (Figure 2G) at the expense of CD33$^+$, CD123$^+$, CD235a$^+$ or CD41$^+$ populations (*Online Supplementary Figure S3E*, summary in Figure 2H).

Cells that formed CFU-M generated by CMML iPSC did not show the typical, fibroblast-like shape of macrophages generated by healthy donor-derived iPSC (Figure 3A, B) and expressed less CD16 and CD163 than

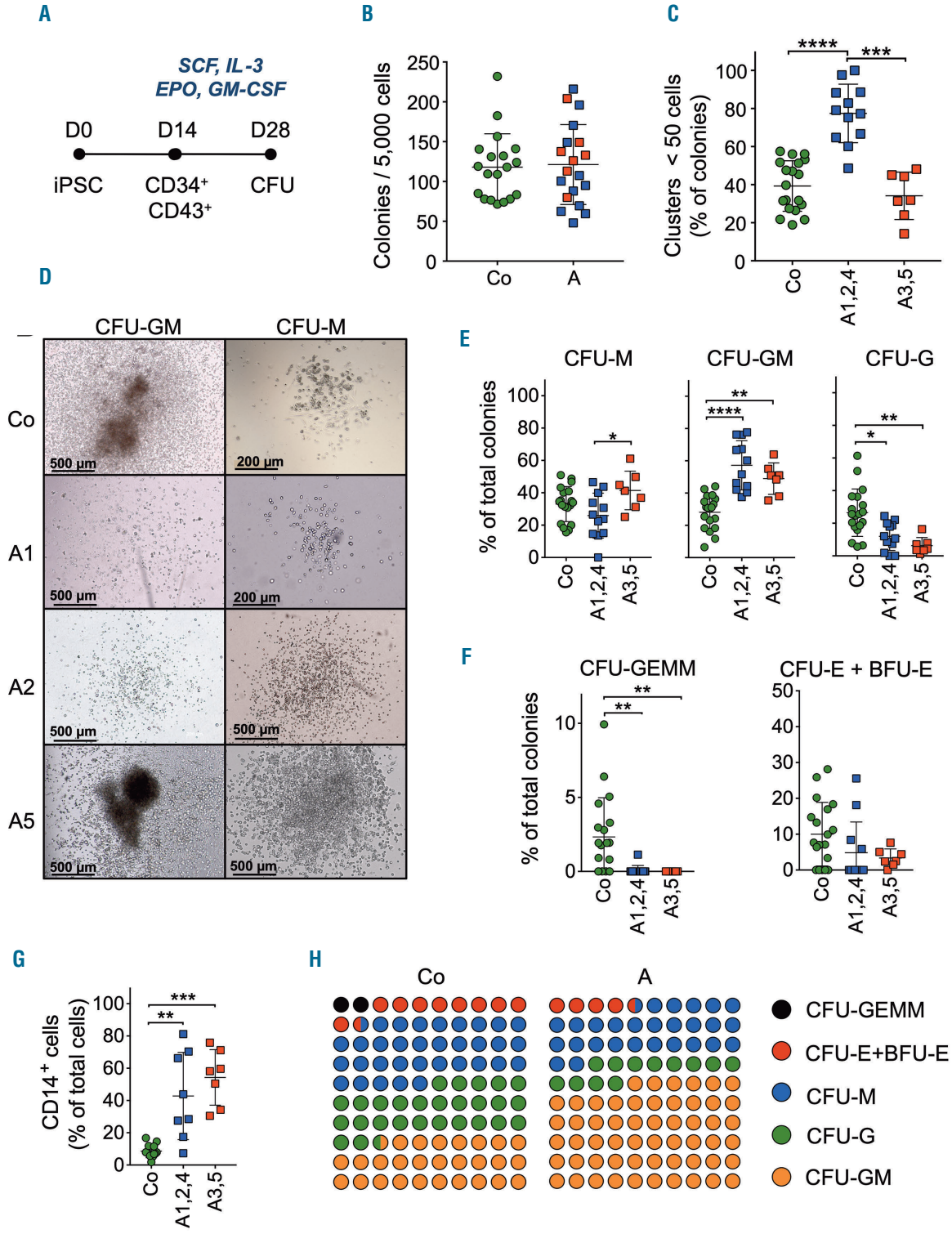

Figure 2. Hematopoietic cells derived from chronic myelomonocytic leukemia induced pluripotent stem cells are biased toward the monocytic lineage. (A) $CD34^+CD43^+$ hematopoietic stem cells derived from control and chronic myelomonocytic leukemia (CMML) induced pluripotent stem cells (iPSC) were sorted and plated for 14 days in methylcellulose in the presence of 50 ng/mL stem cell factor (SCF), 10 ng/mL interleukin-3 (IL-3), 1 U/mL erythropoietin (EPO), and 10 ng/mL granulocyte-macrophage colony-stimulating factor (GM-CSF) before analyzing the generated colonies (CFU). (B) Total number of colonies generated by plating 5,000 cells in methylcellulose for 14 days. Co and A represent the five control and five patient's clones respectively. (C) Fraction of clusters, as defined by colonies <50 cells, among total colonies, separating results obtained with *KRAS*v-wildtype (A1, A2, A4) and *KRAS*-mutated (A3, A5) iPSC; Kruskal-Wallis test. (D) Representative colony-forming unit – granulocyte-macrophage (CFU-GM) and colony-forming unit – macrophage (CFU-M) generated by the indicated clones and visualized by light microscopy. Scale bars indicate magnification. (E) Fractions of CFU-M, CFU-GM and colony-forming unit – granulocyte (CFU-G) among colonies; Kruskal-Wallis test. (F) Fractions of erythroid colonies (CFU-E: colony-forming unit - erythroid; BFU-E: burst-forming unit - erythroid) and CFU-GEMM (colony-forming unit - granulocyte-erythroid-monocyte-megakaryocyte) among colonies; Kruskal-Wallis test. (G) Flow cytometry analysis of $CD14^+$ cells in colonies generated by the indicated clones in methylcellulose; Kruskal-Wallis test. (H) Summary of the colonies generated by hematopoietic progenitors derived from five healthy donor and five CMML patient's iPSC. (B, C, E-G) Green dots, control iPSC; blue squares, *KRAS* wildtype CMML-iPSC; red squares, *KRAS*(G12D) CMML iPSC; bars, mean ± standard deviation. **P*<0.05; ***P*<0.01; ****P*<0,001 *****P*<0.0001.

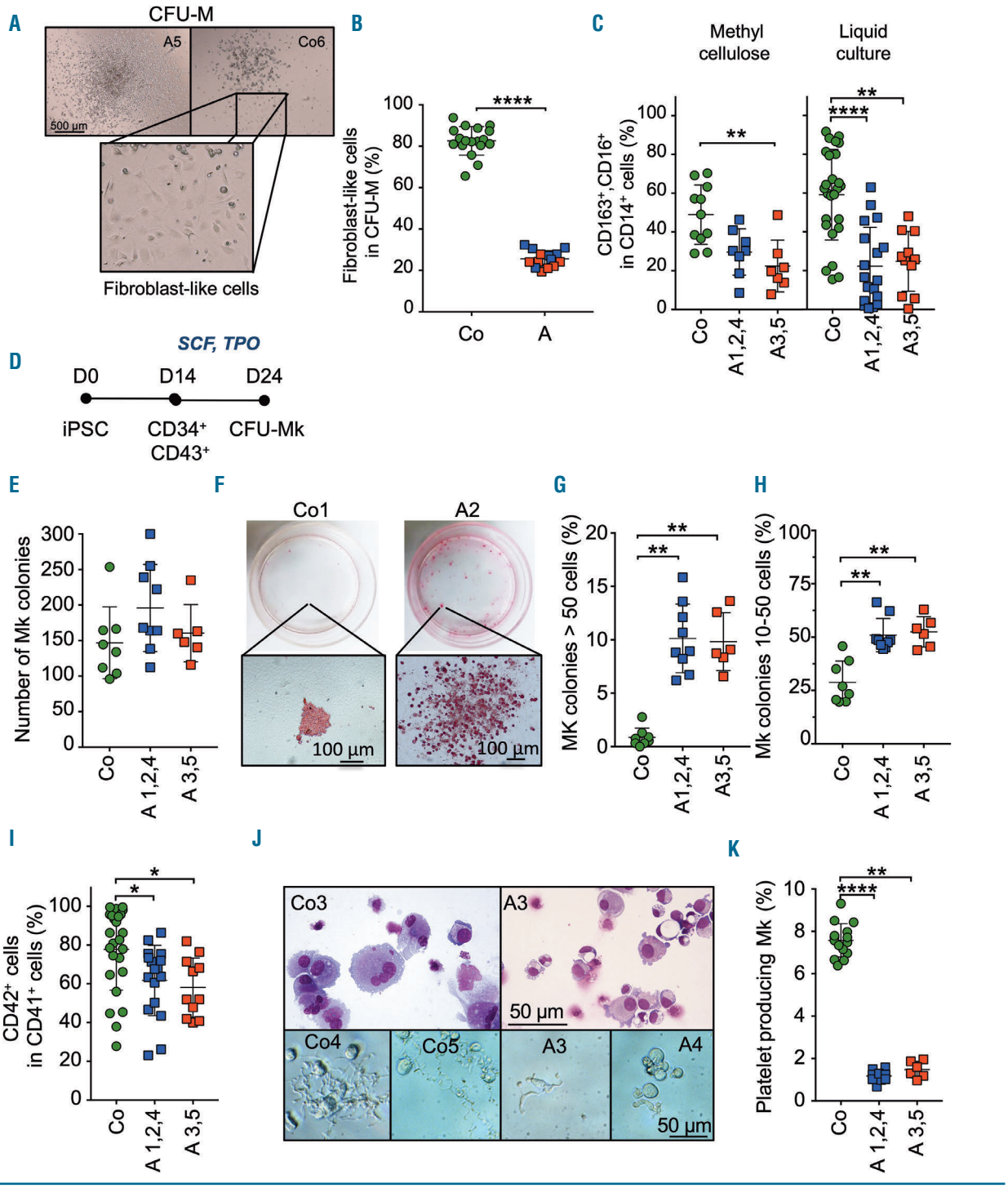

Figure 3. Defective maturation of chronic myelomonocytic leukemia induced pluripotent stem cell-derived hematopoietic cells into macrophages and platelet-forming megakaryocytes. (A) Representative morphology of colony-forming unit – macrophage (CFU-M) generated by hematopoietic cells derived from control (Co6) and chronic myelomonocytic leukemia (CMML) (clone A5) induced pluripotent stem cells (iPSC) cultured in methylcellulose as described in Figure 2A. Light microscopy visualization; scale bar indicates magnification. The rectangle is a zoom on the fibroblast-like shape of macrophages in the Co6 culture, which was not observed in A5 colonies. (B) Fraction of cells with a fibroblast-like shape in CFU-M generated from hematopoietic cells derived from four control and five CMML iPSC; unpaired *t* test. (C) Flow cytometry analysis of cells expressing both CD16 and CD163 in CD14$^+$ cells collected from colonies generated by the five control iPSC- and the five CMML iPSC-derived hematopoietic cells plated in methylcellulose or in liquid medium, Kruskal-Wallis test. (D) Control iPSC and CMML iPSC-derived CD34$^+$CD43$^+$ hematopoietic cells were sorted and plated in coagulum for 10 days in the presence of 50 ng/mL stem cell factor (SCF) and 10 ng/mL thrombopoietin (TPO) to generate colony-forming unit - megakaryocyte (CFU-Mk). (E) Total number of colonies generated by plating 1,500 hematopoietic cells derived from the indicated iPSC. (F) Representative experiments showing the differential morphology of CFU-Mk generated by plating healthy donor (Co1 clone) or CMML (A2 clone) iPSC-derived hematopoietic cells (scale bar, 100 µm). (G) Fractions of large colonies, >50 cells, among the total number of colonies shown in panel E; Kruskal-Wallis test. (H) Fractions of intermediate colonies, 10-50 cells, among the total number of colonies shown in panel E; Kruskal-Wallis test. (I) Fractions of CD41$^+$ megakaryocytes generated in liquid culture with all cytokines for 10 days and expressing the cell surface marker CD42, as detected by flow cytometry; Kruskal-Wallis test. (J) Upper panels show May-Grünwald-Giemsa-stained cytospins of CD41$^+$ cells generated in liquid culture, 5 days after cell sorting, with a normal (Co3) or dysplastic (A3) morphology. Lower panels: representative images of platelet-producing megakaryocytes generated by hematopoietic cells derived from indicated clones; scale bars, 50 µm. (K) Fractions of platelet-producing megakaryocytes in CD41$^+$ cells sorted from liquid culture of CD34$^+$CD43$^+$ cells with all cytokines for 10 days, then cultured for 6 days with SCF and TPO; Kruskal-Wallis test. Mk: megakaryocytes. Colors as in Figure 1. Bars: mean ± standard deviation. *P<0.05; **P<0.01; ****P<0.0001.

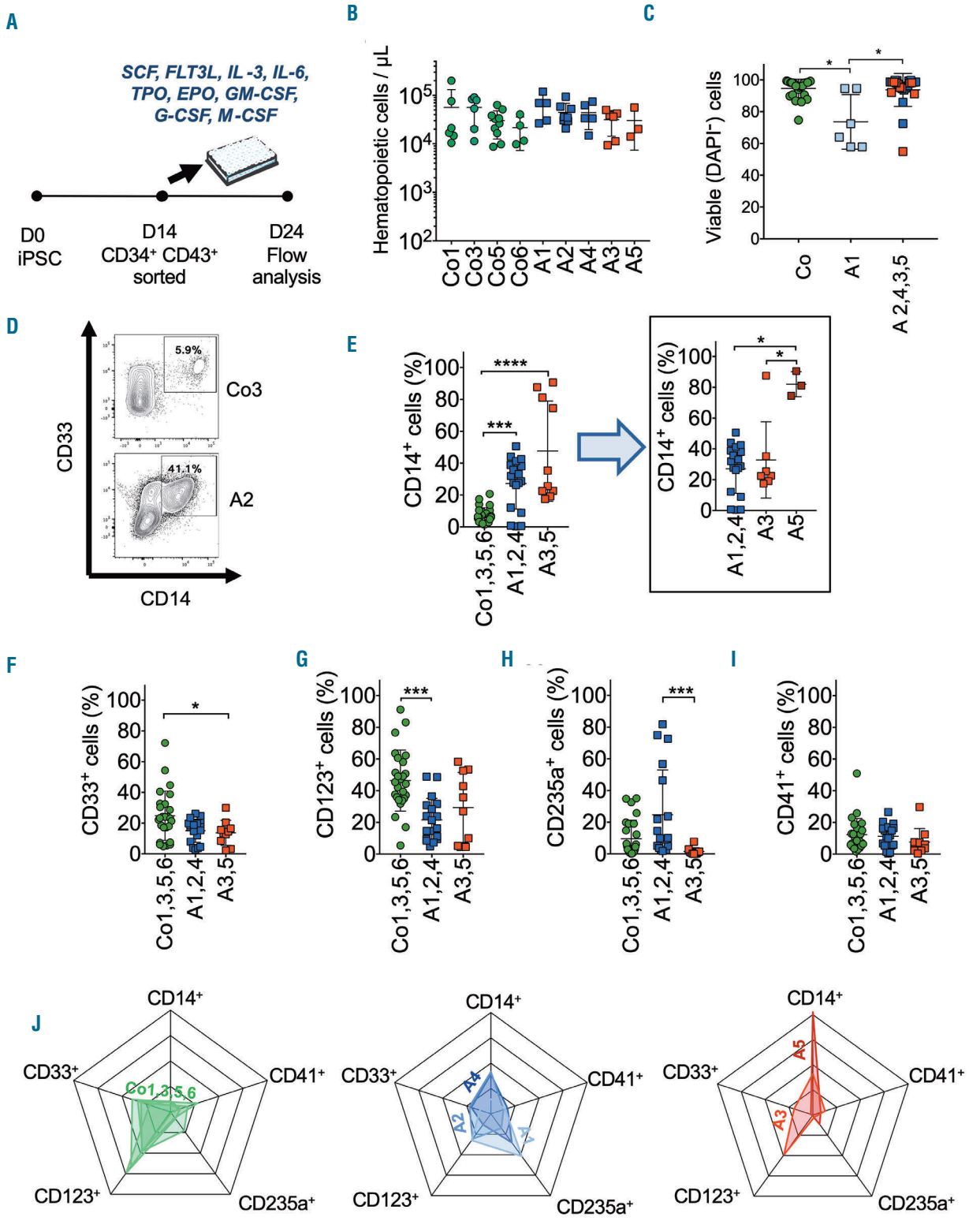

Figure 4. Functional heterogeneity of the patient's induced pluripotent stem cell-derived hematopoietic cells. (A) Control and chronic myelomonocytic leukemia (CMML) induced pluripotent stem cell (iPSC)-derived CD34$^+$CD43$^+$ cells were cultured in liquid medium for 10 days in the presence of 50 ng/mL stem cell factor (SCF), 10 ng/mL Fms-like tyrosine kinase 3 ligand (FLT3L), 10 ng/mL interleukin-3 (IL-3), 10 ng/mL interleukin-6 (IL-6), 50 ng/mL thrombopoietin (TPO), 1 U/mL erythropoietin (EPO), 10 ng/mL granulocyte-macrophage colony-stimulating factor (GM-CSF), 10 ng/mL granulocyte colony-stimulating factor (G-CSF), and 10 ng/mL monocyte colony-stimulating factor (M-CSF). (B) Total number of hematopoietic cells generated by 5,000 CD34$^+$CD43$^+$ cells cultured in liquid medium for 10 days. (C). Fractions of viable, DAPI-negative cells measured on day 10; Kruskal-Wallis test. (D) Representative flow cytometry analysis of CD33$^+$CD14$^+$ cells generated in liquid culture by the Co3 and A2 clones. (E-I) Fractions of CD33$^+$CD14$^+$ cells (E and insert), CD33$^+$CD14$^-$CD41$^-$ cells (F), CD123$^+$CD33$^-$CD235a$^-$CD14$^-$CD41$^-$ cells (G), CD235a$^+$CD14$^-$CD41$^-$ cells (H), and CD41$^+$CD14$^-$ cells (I) generated in liquid culture by the indicated clones; Kruskal-Wallis test. (J) Radar representation of the differentiation potential of CD34$^+$CD43$^+$ hematopoietic cells derived from control iPSC (green), *KRAS* wildtype CMML iPSC (blue) and *KRAS*(G12D) CMML iPSC (red). Bars: mean ± standard deviation. *P<0.05; ***P<0,001 ****P<0.0001

those from control iPSC-derived CFU-M (Figure 3C). A similar defect in the generation of CD14$^+$ cells expressing both CD16 and CD163 was detected when iPSC-derived hematopoietic cells were induced to differentiate in liquid culture (Figure 3C).

Since the patient demonstrated megakaryocytic hyperplasia and dysplasia, we performed coagulum assays in the presence of stem cell factor and thrombopoietin to analyze the generation of megakaryocytes and platelets (Figure 3D). All iPSC generated a similar number of colonies (Figure 3E) but those generated by CMML iPSC were much larger (Figure 3F-H). We observed a decrease in the fraction of CD42$^+$ cells among CD41$^+$ cells (Figure 3I) and the fraction of CMML iPSC-derived megakaryocytes that produced platelets was decreased (Figure 3J, K).

CD34$^+$CD43$^+$ cells generated from iPSC were also cultured in liquid medium in the presence of stem cell factor, interleukin-3, interleukin-6, erythropoietin, granulocyte-macrophage colony-stimulating factor, thrombopoietin, Fms-like tyrosine kinase 3 ligand, granulocyte colony-stimulating factor and monocyte colony-stimulating factor for 10 days (Figure 4A). The quantity of cells generated by each clone and the number of viable cells after 10 days were not significantly different, except for clone A1 that demonstrated more dead cells (Figure 4B, C). Multiparameter flow cytometry analysis was used to measure each cell population obtained in culture (*Online Supplementary Figure S2B*). CMML iPSC generated a majority (~40%) of CD14$^+$ cells (Figure 4D, E). Although they both had a *KRAS*(G12D) mutation, the A5 clone generated more CD14$^+$ cells (~80%) than the A3 clone. In fact, monocyte production by the A3 clone was not significantly different from that of *KRAS* wildtype clones (Figure 4E, insert). Compared to control clones, *KRAS*(G12D) CMML iPSC generated fewer CD33$^+$, CD14$^-$, CD41$^-$, CD235a$^-$ cells (Figure 4F) and *KRAS* wildtype CMML clones generated fewer CD123$^+$, CD14$^-$, CD41$^-$, CD235a$^-$ cells (Figure 4G). The generation of CD235a$^+$ erythroid cells was more heterogeneous and higher in *KRAS* wildtype compared to *KRAS*(G12D) CMML clones (Figure 4H). The generation of CD41$^+$ cells was not significantly different between control and patient-derived iPSC (Figure 4I). These liquid cultures also revealed the defective differentiation of monocytes into macrophages (Figure 3C) and the defective generation of platelets (Figure 3D).

As expected, patient-derived clones showed a bias in their differentiation towards monocyte production. However, hematopoietic differentiation of CMML iPSC also demonstrated significant intraclonal heterogeneity that could not be explained by the sole genetic alterations detected in coding regions. The A1, A2 and A4 clones, which have the same mutations in coding regions, showed heterogeneous differentiation into CD235a$^+$ and CD14$^+$ cells whereas A3 and A5, which are *KRAS*-mutated clones, showed a marked difference in their monocytic differentiation in liquid culture. A summary of this clonal heterogeneity is shown in Figure 4J.

While the viability of cells generated by control iPSC was high in all but one experiment, the viability of CMML iPSC, especially *KRAS* wildtype CMML iPSC, was much more heterogeneous than that of control clones, suggesting a higher sensitivity to small variations in culture conditions (Figure 5A). Of note, the number of generated cells (indicated by the diameter of the circles in Figure 5A) could remain high in cultures in which the cell death rate was elevated. In contrast, a decrease in cell viability was associated with an increase in the fraction of CD235a$^+$ cells and a decrease in the fraction of CD14$^+$ cells generated by *KRAS* wildtype CMML iPSC (Figure 5A). By eliminating this culture condition-related variability in cell production, using a cut-off of 90% viability, we observed a much more robust trend in the differentiation of A1, A2 and A4 clones (*Online Supplementary Figure S4*). In contrast, even with this cut-off on viability, the A5 clone consistently produced more CD14$^+$ cells than the A3 clone (Figure 5B).

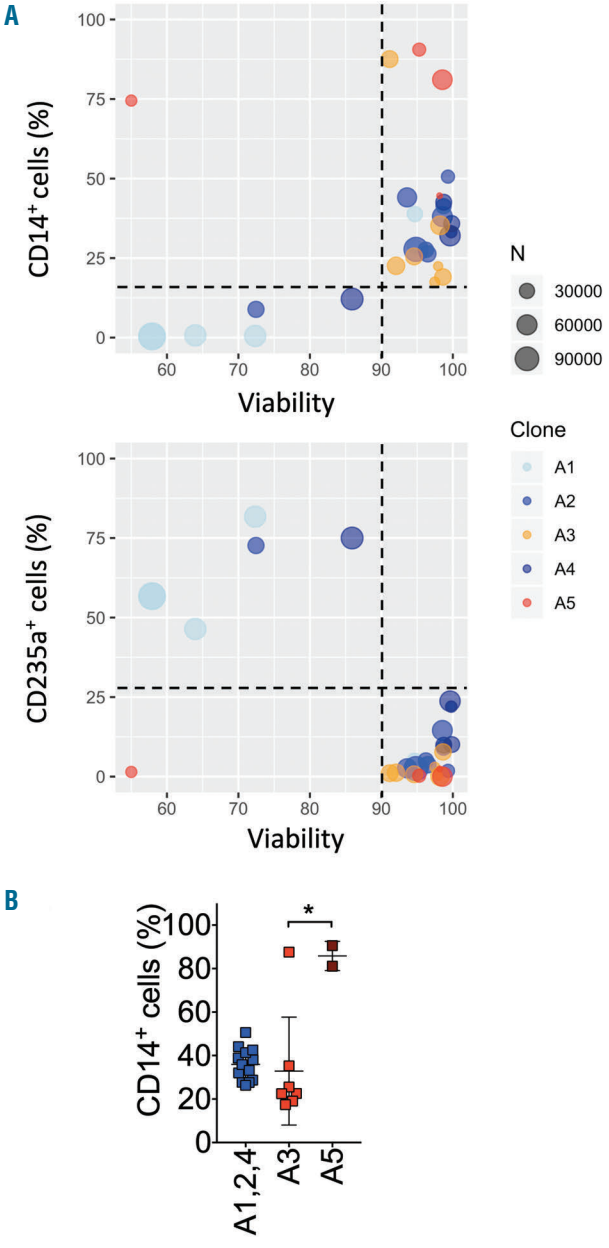

Figure 5. Impact of viability on differentiation pattern analysis. (A) Percentages of DAPI-negative viable cells (x axis) and numbers of hematopoietic cells generated (dots size) are plotted against the fraction of CD14$^+$ and CD235a$^+$ cells generated in liquid culture. The vertical hatched line is an arbitrary cut-off value established at 90% viable cells; the horizontal hatched line emphasizes the discrepancies between samples with <90% viable cells and the others. (B) Fractions of CD33$^+$CD14$^+$ cells for the indicated clones after removing experiments in which cell viability was below 90%; Kruskal-Wallis test. *P<0.05.

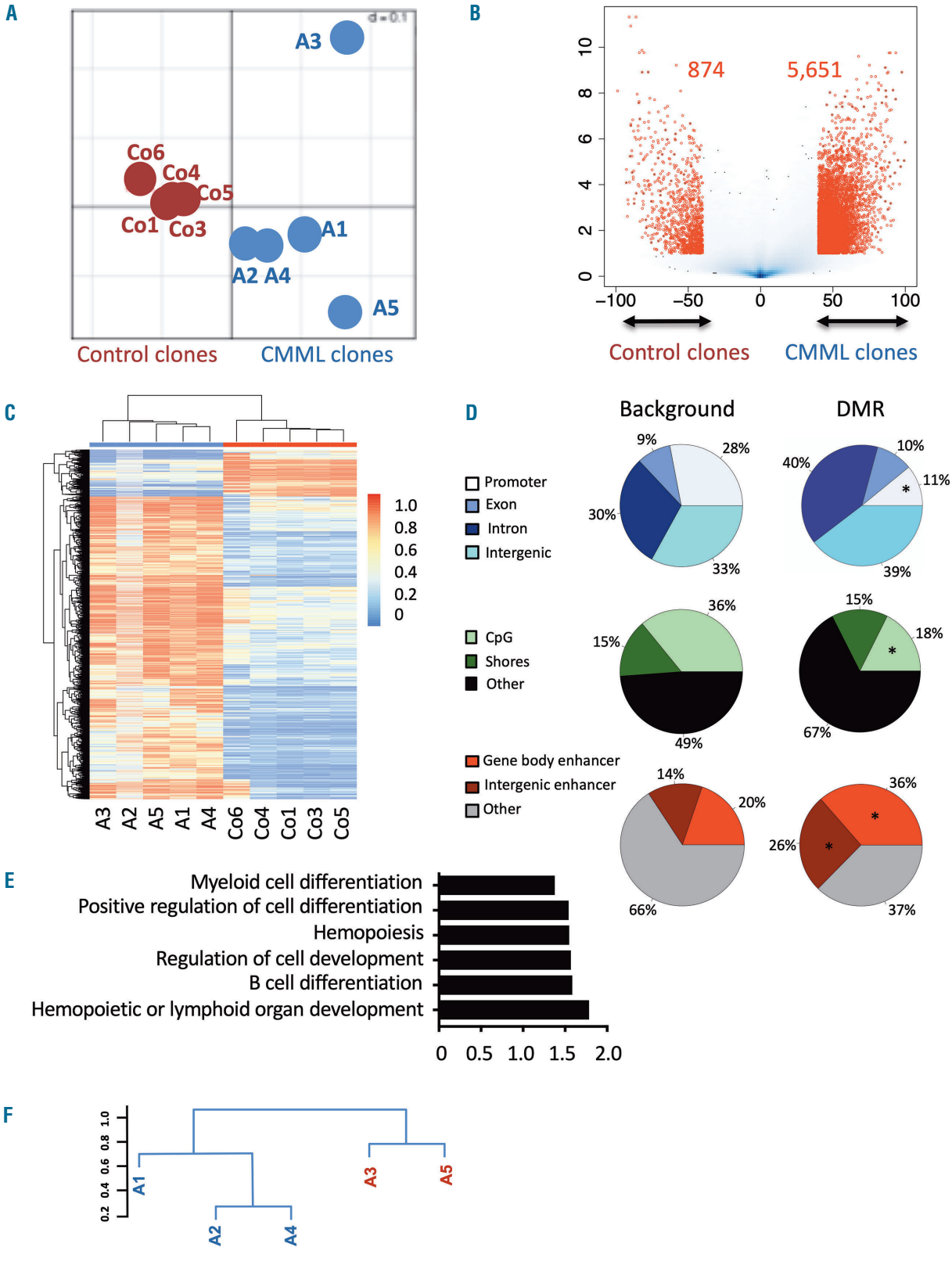

Figure 6. Methylation profile recapitulates features related to the biology of the chronic myelomonocytic leukemia clones. (A) Unsupervised clustering by correspondence analysis showing a clear separation between control, 'Co', and chronic myelomonocytic leukemia (CMML) clones 'A', using tiles with a standard deviation (SD)>0.03. (B) Supervised analysis (β binomial model) displayed a clear trend toward hypermethylation in CMML clones compared to Co clones. Arrows, percentage of methylation required to be considered as a differentially methylated region (DMR). Red dots, tiles that fulfill the criteria [absolute methylation difference ≥40% and false discovery rate (FDR) <5%]. (C) Heatmap of DMR based on the Euclidean distance matrix. Red, hypomethylation; blue, hypermethylation; gray, DMR that were not covered by enhanced reduced representation bisulfite sequencing in a specific tile. (D) Annotation to genomic regions of background of all tiles (left) and DMR (right). Asterisk, significance according to the binomial test (P<0.001). (E) Gene ontology of DMR methylated on CMML clones. Bar chart: processes related to hematopoiesis with a FDR <0.1. X-axis, -$\log_{10}$ of the FDR. (F) Hierarchical cluster of methylation tiles with the highest SD (SD>0.03). Y-axis, distance metric obtained from the Euclidean distance matrix.

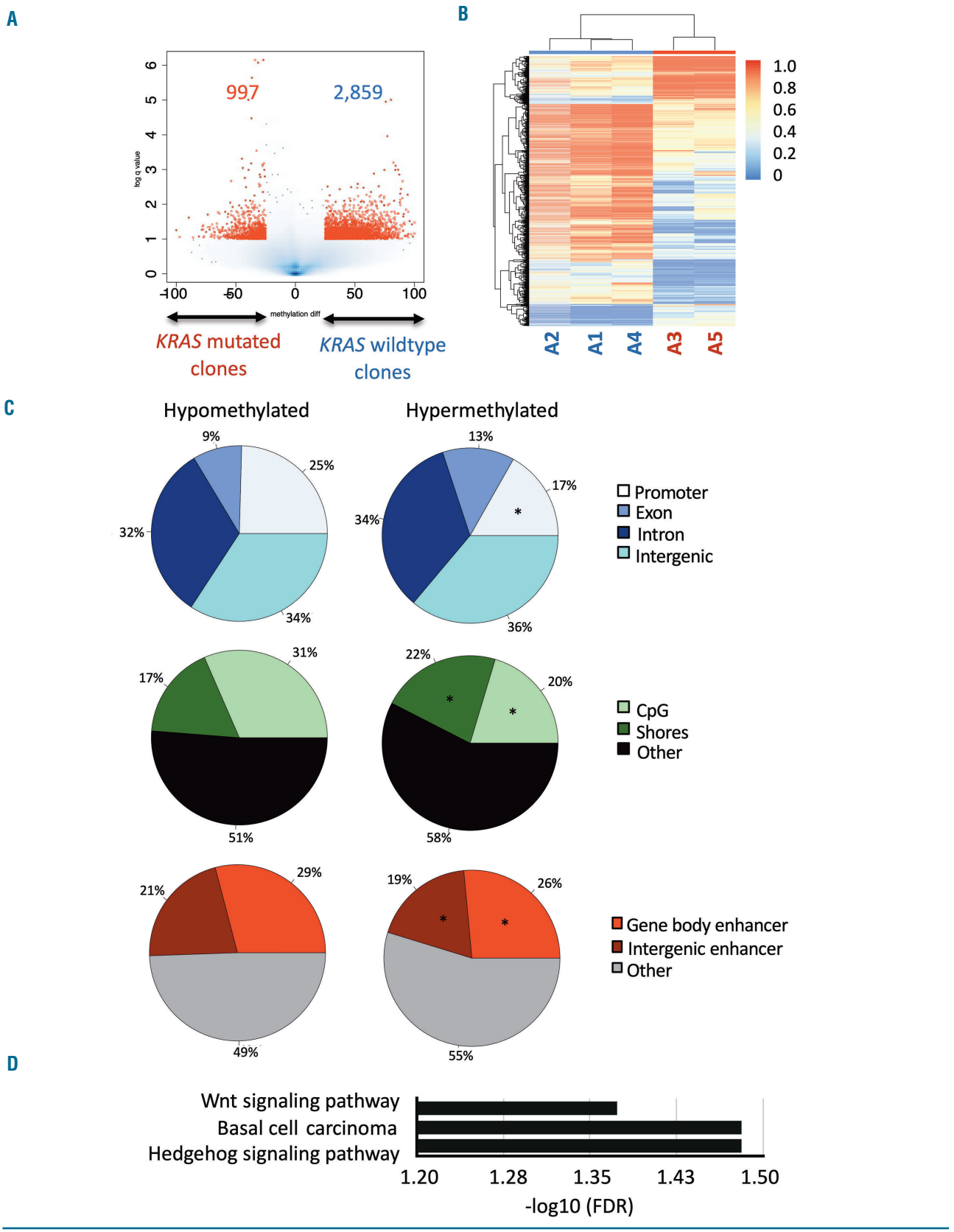

Figure 7. Differential methylation profile of *KRAS*-wildtype and *KRAS*-mutated chronic myelomonocytic leukemia clones. (A) Hypermethylated regions detected by enhanced reduced representation bisulfite sequencing in *KRAS* wildtype (A1, A2, A4) compared to *KRAS* mutated (A3, A5) chronic myelomonocytic leukemia (CMML)-derived induced pluripotent stem cells (iPSC). Arrows, percentage of methylation required to be considered as a differentially methylated region (DMR). Red dots, tiles that fulfill the criteria [absolute methylation difference ≥40% and false discovery rate (FDR) <5%]. (B) Heatmap of DMR based on the Euclidean distance matrix. Red, hypomethylation; blue, hypermethylation; (C) Repartition of DMR that are hypo- or hyper-methylated in *KRAS* wildtype compared to *KRAS*(G12D) clones. Asterisk, significance according to the binomial test (P<0.001). (D) Gene ontology of DMR methylated on *KRAS*(G12D) clones. Bar chart: processes related to hematopoiesis with a FDR <0.1. X-axis, -$\log_{10}$ of the FDR.

Epigenetic heterogeneity among induced pluripotent stem cell clones from the patient with chronic myelomonocytic leukemia

Epigenetic intraclonal heterogeneity has been reported in hematologic malignancies[2,19] as well as in solid tumors,[20] and co-dependency between epigenetic and genetic evolution has been questioned, e.g., in large B-cell lymphoma[21] and acute myeloid leukemia.[3] We performed DNA methylation analysis on $CD34^+CD43^+$ cells generated from iPSC to investigate their epigenetic state. Unsupervised analysis by correspondence analysis separated control- from CMML-derived cells. The latter showed a much greater diversity (Figure 6A). We then used a β binomial model implemented in methylSig[22] to perform a supervised analysis of differentially methylated regions (DMR). We identified 5,651 hypermethylated DMR in CMML-derived cells compared to controls. In contrast, only 874 DMR were identified as more methylated in control iPSC-derived cells (Figure 6B, C). Genomic annotation revealed that, in CMML samples, DMR were depleted at promoter regions and CpG islands while being enriched at gene body and intergenic enhancers (P<0.001 in all cases) (Figure 6D). DMR detected at CpG islands, gene body enhancers and intergenic enhancers were significantly more often hypermethylated regions (P<0.001) (*Online Supplementary Figure S5A*). In accordance with changes in DNA methylation affecting enhancers, we observed significant enrichment of DMR within enhancers[23] compared to background (36.8% at total DMR *vs*. 15.2% background, P-value $<2.2\times10^{-16}$). Motif enrichment analysis suggested that the main sequences targeted by DMR were motifs recognized by transcription factors of the ETS family (*Online Supplementary Figure S5B*). Gene ontology analysis of biological processes of DMR hypermethylated in CMML-derived cells showed enrichment of differentiation and hematopoietic development categories (Figure 6E), suggesting that DNA methylation differences between CMML- and control-derived cells may capture an epigenetic memory related to the biology of the disease, still present after having been reprogrammed. Finally, focusing on CMML iPSC-derived hematopoietic cells, unsupervised hierarchical clustering based on their DNA methylation profiles revealed high concordance with their phylogenetic background (Figure 6F).

In order to correlate changes in DNA methylation with those seen at the expression level, we first looked at the expression status of genes closest to DMR using a nearest gene annotation approach. Using this approach, only 114 genes showed overlapping changes in expression and DNA methylation. However, since focusing on DMR-nearest gene correlations may not correctly capture the three-dimensional nature of gene regulation, we next explored the role of DMR within specific topologically associated domains (TAD) identified using publicly available coordinates. We thus localized each DMR into a given TAD. For every gene within a TAD, we correlated gene expression and methylation levels across the samples using Pearson correlation. With this method, of 196 DMR identified in 66 TAD, we detected changes in gene expression in 72 genes (*Online Supplementary Table S2*).

To further explore the epigenetic differences between subclones of the original disease and the potential contribution of specific mutations to the epigenetic programming, we also compared DNA methylation profiles in *KRAS* wildtype (A1, A2, A4) and *KRAS*(G12D) (A3, A5) clones (Figure 7). Globally, clones that had acquired *KRAS*(G12D) seemed to be relatively hypomethylated compared to the *KRAS* wildtype clones (Figure 7A, B). Acquisition of *KRAS*(G12D) correlated with a new repartition of DMR, including a significant decrease in methylation at intronic regions (P<0.001), CpG shores (P<0.001),

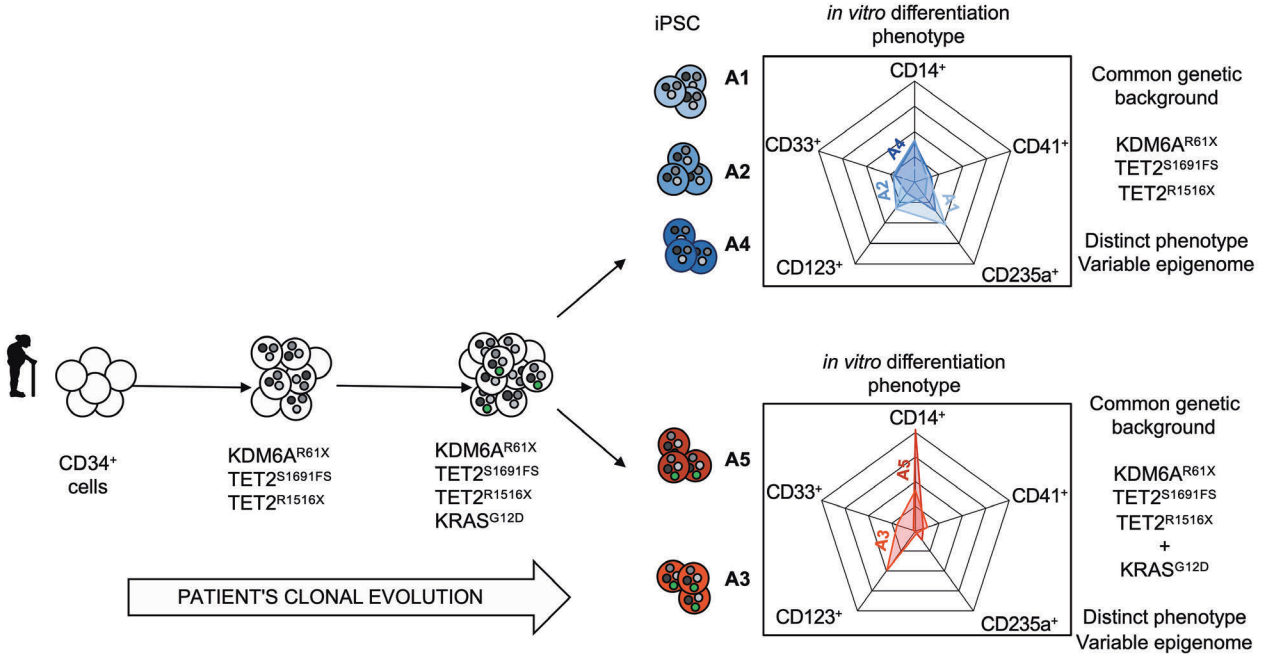

Figure 8. Graphical summary of intratumor heterogeneity layers detected by analysis of five patient-derived induced pluripotent stem cells.

gene body ($P<2.2\ 10^{-16}$) and intergenic enhancers ($P<0.001$) and a significant increase in methylation at promoter regions ($P<0.001$) and CpG islands ($P<0.001$) (Figure 7C). Importantly, using Kyoto Encyclopedia of Genes and Genomes (KEGG) pathway analysis, *KRAS*(G12D) acquisition was shown to induce significant changes in Wnt and Hedgehog signaling pathways, which may indicate a differential role for these pathways in the malignant transformation of the different clones (Figure 7D).

Discussion

The reprogramming of CD34$^+$ cells from a CMML patient generated iPSC whose hematopoietic differentiation recapitulated the main features of the disease while demonstrating functional heterogeneity between clones (see graphical abstract in Figure 8).

Discrepancies between the functional properties of clones sharing a similar genetic background have been reported in organoids derived from colorectal cancer cells.[24] We cannot exclude an effect of recurrent somatic mutations in non-coding regions, as described in some solid tumors,[25] but such events have not been identified yet in CMML cells.[6] A role for cell reprogramming[26,27] in this heterogeneity is also unlikely as control iPSC established independently from two healthy donors had a similar and reproducible behavior, in contrast to the differences observed between genetically identical CMML iPSC (Figure 4J). In addition differences sometimes observed between individual clones derived from the same genotype were shown to pre-exist in the tissue of origin rather than being induced by reprogramming.[28,29] The distinct behavior of CMML-derived iPSC could also reflect intrinsic heterogeneity in CD34$^+$ cell-priming for differentiation.[30,31] If such an intrinsic heterogeneity of CD34$^+$ cell-priming is a general property of CD34$^+$ cells, discrepancies should also have been observed between control iPSC. An alternative explanation is that heterogeneous priming is a specific feature of CMML progenitor cells, which could be related to intraclonal epigenetic heterogeneity. Our epigenetic analyses indicate that, in patient-derived clones, the global pattern of DNA methylation correlates with genetic alterations. However, limited differences in their methylation profiles could possibly account for their functional heterogeneity.

iPSC allow the combined investigation of all levels of intratumoral heterogeneity, from genetic, to epigenetic, to phenotypic and functional properties associated with the disease, offering unique opportunities to study diseases in which functional heterogeneity exceeds genetic heterogeneity, such as CMML.[4] These benefits do, however, come at a cost. As recently reviewed,[15] the derivation of iPSC from patients with a myeloid malignancy to model their disease has to face the relative refractoriness of malignant progenitors to reprogramming, which is in part related to their genetic background and could preclude the capture of intraclonal heterogeneity as some subclones may be reprogrammed more easily than others. The dysplastic nature of these cells, which often correlates with an increased sensitivity to apoptosis, is another challenge to overcome. Lastly, in the patients, the heterogeneous behavior of individual cells may be further influenced by clonal interference and non-cell-autonomous factors,[32] contributing to the diversity of CMML phenotypic traits, and accounting for the current failure of treatments aiming at eradicating the malignant clone.

Acknowledgments

The authors would like to thank Dr Weiss for kindly providing a control iPSC clone. This work was supported by grants from the Ligue Nationale Contre le Cancer (équipe labelisée), Institut National du Cancer (INCA_8073; PRT-K 16-047), Fondation ARC (to AB), Cancéropole Ile de France (emergence program to LL), Siric SOCRATE (INCa-DGOS-INSERM_12551), Molecular Medicine in Oncology program (Agence Nationale de la Recherche), Gustave Roussy Cancer Center (taxe d'apprentissage), the University of Miami Sylvester Comprehensive Cancer Center, the Sylvester Comprehensive Cancer Center Onco-Genomics Shared resource, and the John P. Hussman Institute for Human Genomics, Center for Genome Technology at the University of Miami Miller School of Medicine.

References

1. McGranahan N, Swanton C. Clonal heterogeneity and tumor evolution: past, present, and the future. Cell. 2017;168(4): 613-628.
2. Landau DA, Clement K, Ziller MJ, et al. Locally disordered methylation forms the basis of intratumor methylome variation in chronic lymphocytic leukemia. Cancer Cell. 2014;26(6):813-825.
3. Li S, Garrett-Bakelman FE, Chung SS, et al. Distinct evolution and dynamics of epigenetic and genetic heterogeneity in acute myeloid leukemia. Nat Med. 2016;22 (7):792-799.
4. Ball M, List AF, Padron E. When clinical heterogeneity exceeds genetic heterogeneity: thinking outside the genomic box in chronic myelomonocytic leukemia. Blood. 2016;128 (20):2381-2387.
5. Deininger MWN, Tyner JW, Solary E. Turning the tide in myelodysplastic/myeloproliferative neoplasms. Nat Rev Cancer. 2017;17(7):425-440.
6. Merlevede J, Droin N, Qin T, et al. Mutation allele burden remains unchanged in chronic myelomonocytic leukaemia responding to hypomethylating agents. Nat Commun. 2016;7:10767.
7. Itzykson R, Kosmider O, Renneville A, et al. Clonal architecture of chronic myelomonocytic leukemias. Blood. 2013;121(12):2186-2198.
8. Solary E, Itzykson R. How I treat chronic myelomonocytic leukemia. Blood. 2017;130 (2):126-133.
9. Meldi K, Qin T, Buchi F, et al. Specific molecular signatures predict decitabine response in chronic myelomonocytic leukemia. J Clin Invest. 2015;125(5):1857-1872.
10. Zhang Y, He L, Selimoglu-Buet D, et al. Engraftment of chronic myelomonocytic leukemia cells in immunocompromised mice supports disease dependency on cytokines. Blood Adv. 2017;1(14):972-979.
11. Yoshimi A, Balasis ME, Vedder A, et al. Robust patient-derived xenografts of MDS/MPN overlap syndromes capture the unique characteristics of CMML and JMML. Blood. 2017;130(4):397-407.
12. Chao MP, Gentles AJ, Chatterjee S, et al. Human AML-iPSCs reacquire leukemic properties after differentiation and model clonal variation of disease. Cell Stem Cell. 2017;20(3):329-344.e7.
13. Kotini AG, Chang CJ, Chow A, et al. Stage-specific human induced pluripotent stem cells map the progression of myeloid transformation to transplantable leukemia. Cell Stem Cell. 2017;20(3):315-328.e7.
14. Taoka K, Arai S, Kataoka K, et al. Using patient-derived iPSCs to develop humanized mouse models for chronic myelomonocytic leukemia and therapeutic drug identification, including liposomal clodronate. Sci Rep. 2018;8(1):15855.
15. Papapetrou EP. Modeling myeloid malignancies with patient-derived iPSCs. Exp Hematol. 2019;71:77-84.
16. Mills JA, Wang K, Paluru P, et al. Clonal genetic and hematopoietic heterogeneity

among human induced pluripotent stem cell lines. Blood. 2013;122(12):2047-2052.
17. Welch RP, Lee C, Imbriano PM, et al. ChIP-Enrich: gene set enrichment testing for ChIP-seq data. Nucleic Acids Res. 2014;42(13):e105-e105.
18. Chang CJ, Kotini AG, Olszewska M, et al. Dissecting the contributions of cooperating gene mutations to cancer phenotypes and drug responses with patient-derived iPSCs. Stem Cell Reports. 2018;10(5):1610-1624.
19. Oakes CC, Claus R, Gu L, et al. Evolution of DNA methylation is linked to genetic aberrations in chronic lymphocytic leukemia. Cancer Discov. 2014;4(3):348-361.
20. Mazor T, Pankov A, Song JS, Costello JF. Intratumoral heterogeneity of the epigenome. Cancer Cell. 2016;29(4):440-451.
21. Pan H, Jiang Y, Boi M, et al. Epigenomic evolution in diffuse large B-cell lymphomas. Nat Commun. 2015;6(1):6921.
22. Park Y, Figueroa ME, Rozek LS, Sartor MA. MethylSig: a whole genome DNA methylation analysis pipeline. Bioinformatics. 2014;30(17):2414-2422.
23. Akalin A, Garrett-Bakelman FE, Kormaksson M, et al. Base-pair resolution DNA methylation sequencing reveals profoundly divergent epigenetic landscapes in acute myeloid leukemia. PLoS Genet. 2012;8(6):e1002781.
24. Roerink SF, Sasaki N, Lee-Six H, et al. Intra-tumour diversification in colorectal cancer at the single-cell level. Nature. 2018;556(7702):457-462.
25. Nault JC, Mallet M, Pilati C, et al. High frequency of telomerase reverse-transcriptase promoter somatic mutations in hepatocellular carcinoma and preneoplastic lesions. Nat Commun. 2013;4(1):2218.
26. Cahan P, Daley GQ. Origins and implications of pluripotent stem cell variability and heterogeneity. Nat Rev Mol Cell Biol. 2013;14(6):357-368.
27. Nishizawa M, Chonabayashi K, Nomura M, et al. Epigenetic variation between human induced pluripotent stem cell lines is an indicator of differentiation capacity. Cell Stem Cell. 2016;19(3):341-354.
28. Kwon EM, Connelly JP, Hansen NF, et al. iPSCs and fibroblast subclones from the same fibroblast population contain comparable levels of sequence variations. Proc Natl Acad Sci U S A. 2017;114(8):1964-1969.
29. Yoshizato T, Dumitriu B, Hosokawa K, et al. Somatic mutations and clonal hematopoiesis in aplastic anemia. N Engl J Med. 2015;373(1):35-47.
30. Naik SH, Perie L, Swart E, et al. Diverse and heritable lineage imprinting of early haematopoietic progenitors. Nature. 2013;496(7444):229-232.
31. Velten L, Haas SF, Raffel S, et al. Human haematopoietic stem cell lineage commitment is a continuous process. Nat Cell Biol. 2017;19(4):271-281.
32. Marusyk A, Tabassum DP, Altrock PM, Almendro V, Michor F, Polyak K. Non-cell-autonomous driving of tumour growth supports sub-clonal heterogeneity. Nature. 2014;514(7520):54-58.